Recep Tayyip Erdoğan Üniversitesi Fen ve Mühendislik Bilimleri Dergisi, 4(2) 65-75 2023
Recep Tayyip Erdogan University Journal of Science and Engineering, 4(2) 65-75 2023
ISSN: 2687-2315 / E-ISSN: 2757-7686

Macro-Porous Aluminum Oxide-Boron Carbide Ceramics for Hard Tissue Applications

Kerim Emre ÖKSÜZ*

*Sivas Cumhuriyet University, Department of Metallurgical and Materials Engineering, Sivas, 58140, Türkiye

*Sorumlu Yazar/Corresponding Author
E-mail: emre.oksuz@cumhuriyet.edu.tr

Araştırma Makalesi/Research Article
Geliş Tarihi/Received:06.05.2023
Kabul Tarihi/Accepted: 06.07.2023

ABSTRACT

This paper focuses on the development of high-quality bioceramic foams for the treatment of hard tissue defects, which are a widespread clinical problem worldwide. In this experimental study, α-alumina (Al_2O_3) ceramics with boron carbide (B_4C) additives, intended for use in biomedical applications, were produced and characterized as highly porous using the replication method. The thermal properties of open-pore polyurethane sponges, with a pore size of 20 ppi, used as an economical polymer model material, were determined by thermo-gravimetric (TGA) and derivative thermogravimetric analysis (DTG). Ceramic foams based on Al_2O_3, with varying B_4C ratios, were obtained by high-temperature sintering and were thoroughly examined using high-resolution field emission gun scanning electron microscopy (FEG-SEM) for homogeneity, high porosity, and interconnected pore microstructure. X-ray diffraction (XRD) analyses confirmed the presence of B_4C within the structure and phase changes. The compressive strength values of sintered ceramic foams containing 0%, 3%, and 5% B_4C by weight were measured as 1.92 MPa, 2.05 MPa, and 2.38 MPa, respectively. In vitro tests were performed to evaluate the biological response that biomaterials intended for use in living environments would produce. Satisfactory results were obtained from cell viability experiments, demonstrating that the addition of B_4C to Al_2O_3-based ceramic foams supports cell proliferation, which is an important advantage in hard tissue defect treatment.

Keywords: Al_2O_3, B_4C, Ceramic foam, In vitro, Macro porous, Microstructure

Sert Doku Uygulamaları için Makro Gözenekli Alüminyum Oksit-Bor Karbür Seramikleri

ÖZ

Bu çalışma, dünya çapında yaygın bir klinik problem olan sert doku defektlerinin tedavisi için yüksek kaliteli biyoseramik köpüklerin geliştirilmesine odaklanmaktadır. Bu deneysel çalışmada, biyomedikal alanlarda kullanılması hedeflenen bor karbür (B_4C) ilaveli α-alüminyum oksit (Al_2O_3) seramikler replika yöntemi ile yüksek gözenekli olarak üretilmiş ve karakterize edilmiştir. Ekonomik polimer model malzeme olarak kullanılan açık gözenekli, 20 ppi gözenek boyutunda poliüretan süngerlerin termogravimetrik (TGA) ve derivatif termogravimetrik analizleri (DTG) ile termal özellikleri belirlenmiştir. Yüksek sıcaklıkta sinterlenerek elde edilen, farklı B_4C oranları içeren Al_2O_3 esaslı seramik köpükler homojen, yüksek gözenekli ve birleştirici gözenek mikroyapısında olduğu yüksek alan emisyon tabancalı taramalı elektron mikroskobu (FEG-SEM) ile detaylı olarak incelenmiştir. X-ışınları (XRD) analizleri ile B_4C'nin yapı içerisinde varlığı ve faz değişimleri doğrulanmıştır. Yapısında ağırlıkça %0, %3 ve %5 B_4C içeren sinterlenmiş seramik köpüklerin basma mukavemeti değerleri sırasıyla 1,92 MPa, 2,05 MPa ve 2,38 MPa olarak ölçülmüştür. Canlı ortamlarda kullanılacak biyomalzemelerin oluşturacağı biyolojik cevabın önceden değerlendirilmesi amacıyla yapılan in vitro testlerde tatmin edici sonuçlar elde edilmiştir. Hücre canlılığı deneyleri, Al_2O_3 esaslı seramik köpüklere B_4C ilavesinin sert doku defektlerinde önemli bir avantaj olan hücre proliferasyonunu desteklediğini göstermiştir.

Anahtar Kelimeler: Al_2O_3, B_4C, Seramik köpük, In vitro, Makro gözenek, Mikroyapı

Cite as;
Öksüz, K.E. (2023). Macro-Porous Aluminum Oxide-Boron Carbide Ceramics for Hard Tissue Applications, *Recep Tayyip Erdogan University Journal of Science and Engineering*, 4(2), 65-75. DOI: 10.53501/rteufemud.1293580

1. Introduction

Biomaterials have been the subject of extensive research due to their capacity to treat bone defects, a common clinical problem that has become more widespread around the world (Xue et al., 2022). Bone defects can arise from various factors such as trauma, cancer, infection, and arthritis (Turnbull et al., 2018). These materials can consist of biometals (Zheng et al., 2020), biopolymers (Luo et al., 2021), bioceramics (Öksüz, 2019), and biocomposites (Özer and Öksüz, 2019). Bioceramic materials, which are made of ceramics that are biocompatible with the body, have a wide range of medical applications and can vary in their level of reactivity with biological tissues, from inert to active (Öksüz et al., 2023). Bioactive materials interact with body tissues through chemical bonding (Silva et al., 2022), while biodegradable bioceramics serve as a temporary scaffold to allow the regeneration of new bone tissue, after which they are naturally replaced by the body without requiring removal surgery (Chen et al., 2021). In contrast, bioinert materials do not have any chemical interaction with the biological environment or the body tissue, but they play a crucial role in bone implants due to their superior mechanical properties and high chemical stability (Kido et al., 2013). Alpha-alumina (α-Al_2O_3) is one of the bioinert bioceramics that has been extensively studied in dental and medical implants for several decades (Ahmed et al., 2020).

Dental bioceramics have gained significant attention due to their biocompatibility, excellent long-term aesthetics, and ability to be shaped precisely. The two most commonly used dental bioceramics are Alumina (Al_2O_3) and Zirconia (ZrO_2), as they exhibit favorable mechanical properties and biocompatibility. Although Al_2O_3 is highly biocompatible and wear-resistant, it possesses low flexural strength and toughness (Marti, 2000). In order to enhance its mechanical properties, two composite materials have been developed by incorporating a second phase (Jang et al., 1995; Öksüz and Özer, 2017) or embedding whisker (Tan et al., 2020) into an Al_2O_3 matrix. B_4C is another promising material with attractive properties such as low density, good wear/corrosion resistance, and extremely high hardness (Tian, 1999; Suri et al., 2010). Moreover, B_4C finds recent applications in medicine, specifically in Boron Neutron Capture Therapy (BNCT) (Yoshie Ishikawa, 2014; Gosset et al., 2016; Mirzayev et al., 2020). The main benefit of B_4C is its abundance of natural boron in the compound, ranging from 80 to 91 at % (Werheit, 2016), which is highly advantageous for BNCT therapy (Gosset et al., 2016; Bute et al., 2016; Barth et al., 2012). The possible application of materials in the medical field is determined by how the powder particles interact with biological materials, including their surface chemistry (Mortensen et al., 2006).

The current experimental study has focused on examining the structural behavior of Al_2O_3-B_4C biocomposites and the impact of B_4C on various properties such as microstructure, grain growth mechanism, pore structure, phase evolution and thermal properties. Additionally, the mechanical and in vitro properties of the biocomposites have also been investigated and assessed.

2. Materials and Methods

2.1. Chemicals and Materials

The commercial Aluminum oxide powder (α-Al_2O_3 > 98.9 %, ≤ 10μm, ρ =3.99 g/cm^3) and commercial Boron carbide powder ($B_4C \geq 99$ %, ≤ 10μm, ρ =2.52 g/cm^3) were purchased from Merck (Germany) and H.C. Stärck (Germany) company respectively. Commercial polyurethane sponges obtained from Ürosan Kimya Sanayi Company (Türkiye) were used. Polyurethane sponges with an open porosity of around 20 pores per inch were selected from commercial sources (D/22 20 PPI ESTER). Polyvinyl alcohol polymer (PVA-$(C_2H_4O)x$; Mw=60.000 g/mol), polyethylene imine (PEI) thickening agent, ammonium polyacrylate dispersing agent (DARVAN® 821-A), were purchased from Sigma-Aldrich (St. Louis, USA). The solvents used were double deionized (dH_2O, resistivity of 18.2 MΩ cm^{-1}) water, 200 proof ethyl alcohol.

The reagents were utilized in their original form without undergoing any additional purification processes. All other in vitro experimental supplies and reagents procured from Merck (Germany), Thermo Fisher Scientific (Massachusetts, USA), and Bayer AG (Leverkusen, Germany) were of analytical quality.

2.2. Preparation of Ceramic Foams

Boron carbide (B_4C) powders at 3 wt. % and 5 wt. %, respectively, were blended with aluminum oxide powders (α-Al_2O_3, 95 wt. %) using a planetary high-energy ball mill (Retsch PM 100-Germany) at room temperature. To ensure adequate blending, a ZrO_2 vessel was filled with Al_2O_3/B_4C powders and ZrO_2 balls and secured onto a high-energy milling device. The powders were then milled at 600 rpm for 3 hours with a *ball*/*powder ratio* of 10:1, to obtain each homogenous compositions separately. To prepare the slurry, PVA was dissolved in dH_2O at 60 °C to obtain 5% (w/v) PVA solution. The PVA solution and Al_2O_3/B_4C ceramic powders were mixed and mechanically stirred at a rate 1400 rpm for 1 hour. PEI and DARVAN® 821-A solution were added to the slurries and mixed for an additional hour to achieve a slurry with 70-80 wt.% solid loading (Han et al., 2002). To create cubic specimens with dimensions of 1 cm x 1.5 cm x 1 cm, high-density polyurethane sponge pieces were cut and immersed in the ceramic slurry. The slurry coated the sponge and filled its voids. After impregnation, the sponge was compressed using parallel plates with a constant gap, expelling approximately 80 % of the ceramic slurry. The sponge coated with the slurry was left to dry for a minimum of 24 hours at room temperature. The resultant samples were dried for a minimum of 12 hours in a muffle furnace at 120 °C. A gradual heating rate of 2 °C per minute was applied to reach a temperature of 600 °C, where water was evaporated and the polyurethane fibers were allowed to vaporize or burn out, while preserving the filamentary structure of the ceramic material. The sintering process was then conducted in air at a heating rate of 5 °C per minute until it reached 1500 °C, and then held for an hour. This allowed the fused ceramic foam to have interconnected voids that were surrounded by a network of bonded or fused foam ceramic filters (Naga et al., 2013). Figure 1 shows the physical and apparent properties of the sintered porous ceramic foams.

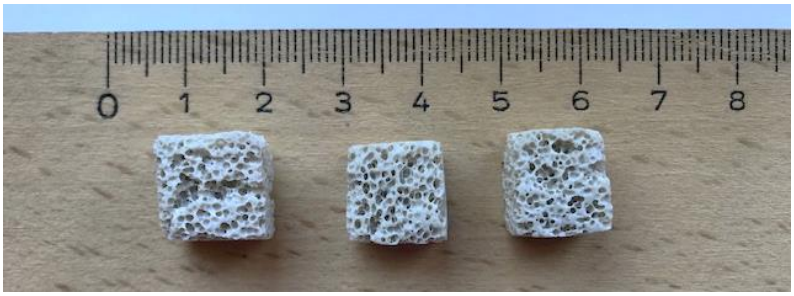

Figure 1. Real photos after sintering of 0 wt.% B_4C, 3 wt.% B_4C and 5 wt.% B_4C reinforced Al_2O_3 based ceramic foams, respectively

2.3. Characterization of Samples

2.3.1. Differential Thermogravimetry Analyses (DTG/TGA)

TGA/DTG analysis is essential for characterizing the thermal behavior, stability, and composition of polymers, enabling researchers and industry professionals to make informed decisions regarding material selection, processing conditions, and product performance. To analyze the thermal and degradation profiles of commercial polyurethane sponges, DTG/TGA was performed using a DTG 60 series TG/DTA thermal analyzer (Schimadzu, Japan). The samples were scanned at a rate of 10 °C min^{-1} in an air atmosphere at temperatures between 50 °C and 650 °C, and measurements were collected over three repeats using a 4 mg sample mass.

2.3.2. Field Emission Gun-Scanning Electron Microscopy (FEG-SEM) Examinations

To analyze the morphologies of the Al_2O_3, $Al_2O_3/3B_4C$ and $Al_2O_3/5B_4C$ ceramic foam samples, field emission gun scanning electron microscopy was used. The FEG-SEM instrument used was the Tescan® Mira3 XMU, Brno, Czechia, with an accelerating voltage of 15-25 kV. To prepare the samples, the foam samples were transferred onto a sample stage with carbon tape conductive film and coated with gold using an ion sputter coater (SCM-200 (Polaris), Republic of Korea).

2.3.3. X-ray Diffraction (XRD) Analysis

XRD analysis was performed using a Cu-Kα diffractometer (Rigaku D/MAX/2200/PC, Japan). The scan range was 10° to 90° with a step size of 0.01° and a speed of 1 s/step. The resulting data were evaluated using computer software (Jade; Materials Data Inc., Livermore, CA) to characterize the crystal structure of the ceramics foams that were sintered was analyzed by comparing the diffractograms with the standards provided by the International Centre for Diffraction Data (ICDD).

2.3.4. Compressive Strength of Samples

Sintered ceramic foams were subjected to compressive strength tests using a universal mechanical testing machine (AGX™-V2 Universal/Tensile testing machine, Schimadzu, Japan) at a crosshead loading speed of 0.5 mm/min. The arithmetic average of data obtained from six samples (n=6) was taken, and the standard deviation was calculated.

2.3.5. In Vitro Cytocompatibility

L929 cells were cultured in DMEM supplemented with 1% (v/v) pre-made penicillin (100 units/mL) and streptomycin (100 units/mL) solution, as well as 10% (v/v) fetal bovine serum (FBS). 1 g of the Al_2O_3, $Al_2O_3/3B_4C$ and $Al_2O_3/5B_4C$ ceramic foam samples were added to 24-well plates, with some wells left empty as controls. L929 cells with a density of $1x10^4$ cells/mL (200 µL) were then added to each well and incubated for 48 hours. Afterward, MTT (3-(4,5-Dimethylthiazol-2-yl)-2,5-Diphenyltetrazolium Bromide) solution (0.5% w/v) and fresh DMEM were added to each well and incubated for 4 hours at 37 °C. OD values of the resulting purple solutions were measured at 490 nm using a Multiskan™ Photometer (Thermo Scientific™, U.S.A.). Triplicate conditions were included in each experiment, and three independent experiments were conducted (Öksüz et al., 2021).

2.3.6. Statistical Analysis

An ANOVA method followed by a post-hoc Tukey test was employed to conduct statistical analysis, and a significance level of $p < 0.05$ was applied to establish statistical significance. The data were marked with * to denote $p < 0.05$ and ** to indicate $p < 0.01$.

3. Results and Discussion

3.1. Thermal Stability of Polyurethane (PU) Sponges

Figure 2a and Figure 2b present the thermogravimetric analysis (TGA), differential thermogravimetry (DTG) analysis curves for commercial PU foams. The decomposition onset temperature (T_{onset}), designed as the temperature at which the sample loss 5 wt.% weight, and the temperature at which the sample has the maximum degradation rate (T_{max}) for rigid PU foams were determined as 285.5 °C and 357 °C respectively. As depicted in Figure 2a, the TGA thermogram indicates that heating triggered two degradation phases. The initial phase, at 285.5 °C, possibly relates to the breakdown of urethane bonds, whereas the second phase, at 357 °C, may be due to the decomposition of polyol esters (sharp peak in Figure 2b) (Sulyman et al., 2021).

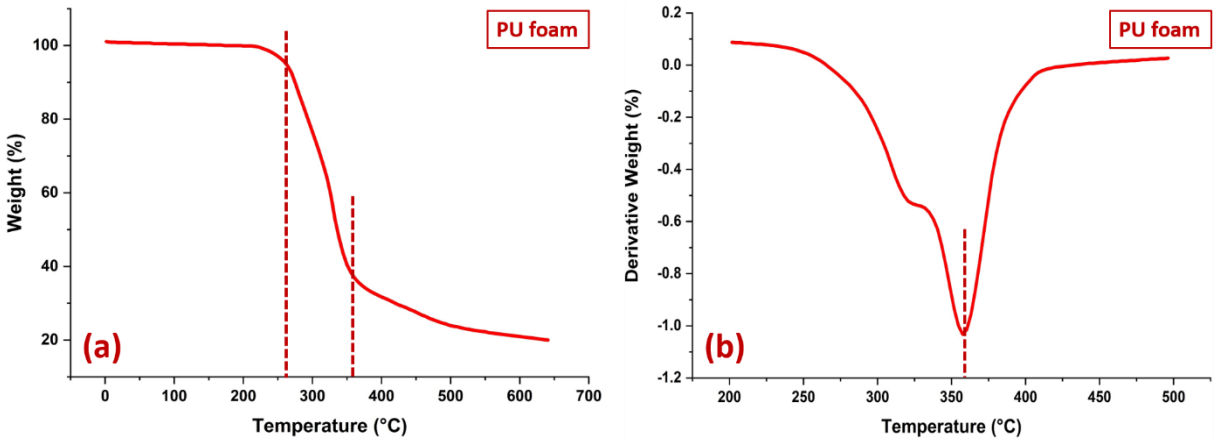

Figure 2. (a) TGA and DTG (b) curves of pure PU foams

3.2. Micro and Macrostructure of Al_2O_3-B_4C Ceramic Foams

Figure 3 presents the macro and micro structures of sintered ceramic foams that have been reinforced with varying amounts of B_4C. These foams are composed of a 3D array of struts with polyhedral cells that exhibit preferential orientation in the direction of polyurethane rise. Some cell windows are covered with a thin ceramic membrane, while the struts and pore walls consist of well-sintered ceramic foam material with a pore size of 1-1.5 mm. The microstructure of the ceramic foams may display some typical defects such as triangular voids inside struts and long cracks between walls (Oliveira et al., 2006).

All samples have been found to possess completely open porosity with interconnected pores. The pore size, evenly distributed pores, interconnectivity of pores, and the ability to facilitate the growth of newly formed hard tissues and cell migration are crucial factors to consider in obtaining macroporous scaffolds (Wu et al., 2021).

Upon close inspection using high magnification FEG-SEM photographs, it is evident that ceramic foams produced without B_4C additives have different grain sizes than those with B_4C additives. The intercept method was used to analyze the grain size evolution, and the average grain size of Al_2O_3 ceramic foam was approximately 6.75 µm, while that of Al_2O_3/$3B_4C$ and Al_2O_3/$5B_4C$ was approximately 6.22 µm and 5.46 µm, respectively. The addition of B_4C to Al_2O_3 matrix during sintering can act as a grain growth inhibitor, effectively retarding grain growth in Al_2O_3 matrix by inhibiting the migration of grain boundaries and nucleation of new grains (Akbari beni et al., 2014). Incorporating 3 wt.% to 5 wt.% B_4C in Al_2O_3 during sintering at 1500 °C may aid in limiting the growth of Al_2O_3 grains, resulting in a finer microstructure and improved mechanical properties. Furthermore, the greater hardness of B_4C compared to Al_2O_3 likely contributed to grinding during mechanical activation, resulting in a finer grain size.

3.3. X-ray Diffraction (XRD) Analysis

The XRD patterns of the as-prepared ceramic foams in Figure 4 prove that B_4C-reinforced Al_2O_3 ceramic foams are successfully prepared by this process. It is observed that for the sintered ceramic foams at 1500 °C for 1 hour, all the intensive peaks correspond to Al_2O_3 (JCPDS: 01-075-1865), whereas less intense ones correspond to B_4C (JCPDS: 00-001-1163). Additionally, new small peaks appear, indicating the formation of B_4C in Al_2O_3/$3B_4C$ and Al_2O_3/$5B_4C$ ceramic foam samples. The obtained XRD patterns clearly indicate that the dissolved and high-energy milled B_4C particles react with Al_2O_3, confirming the effective incorporation of B_4C into the Al_2O_3 matrix. Furthermore, the X-ray analyses show that upon adding B_4C to the Al_2O_3 matrix, the corresponding peaks exhibit a slight expansion, which suggests that the B_4C particles penetrate into the matrix. It is worth mentioning that no

traces of undesirable phases were observed in the XRD patterns during the sintering process. This confirms the high purity of the resulting B_4C-reinforced Al_2O_3 ceramic foams, which are suitable for various applications in fields such as tissue and biomedical engineering.

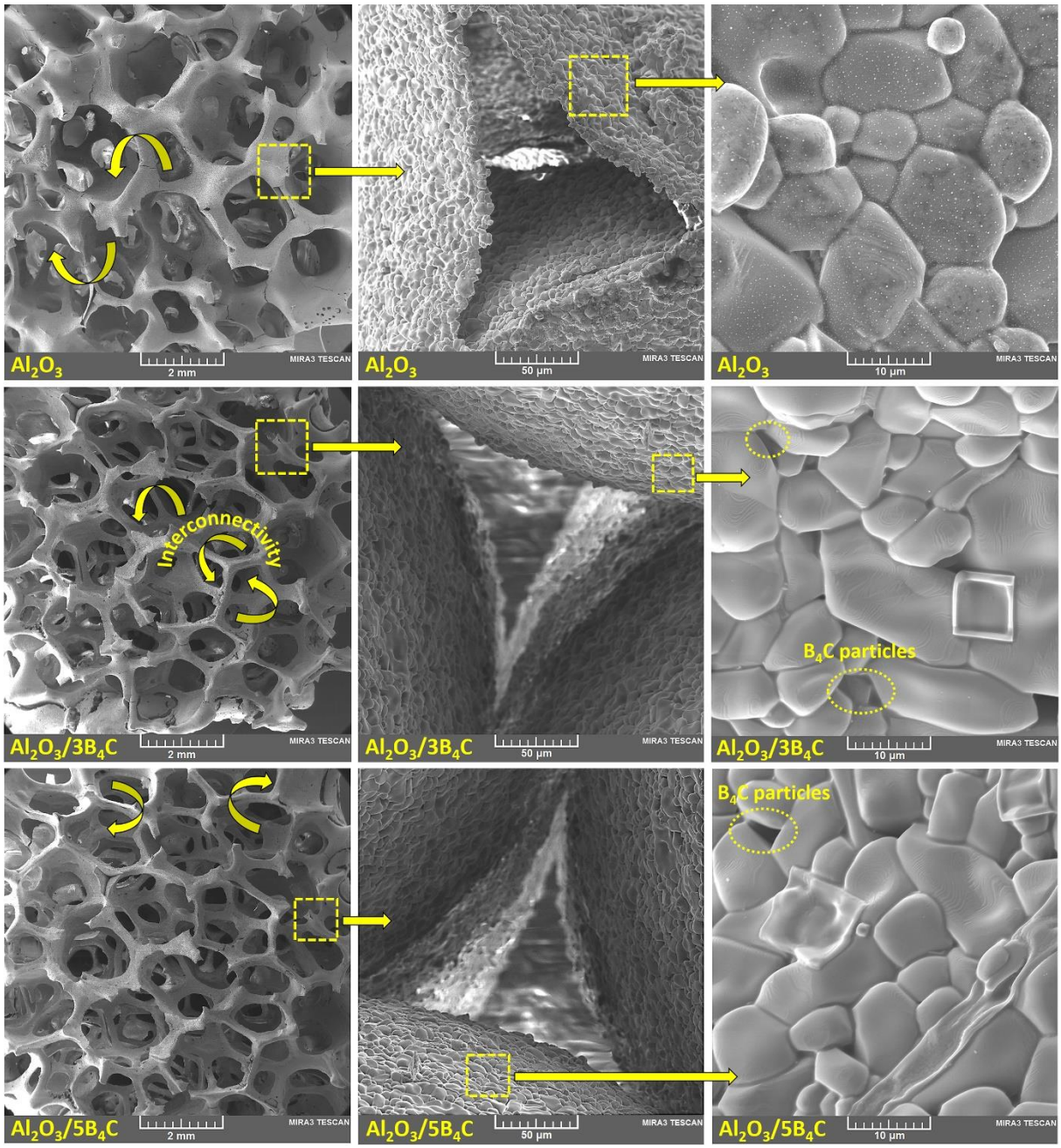

Figure 3. (a) FEG-SEM images of surface morphology and pore structure of Al_2O_3 based ceramic foams, and magnified images of pore ridge and pore wall surface

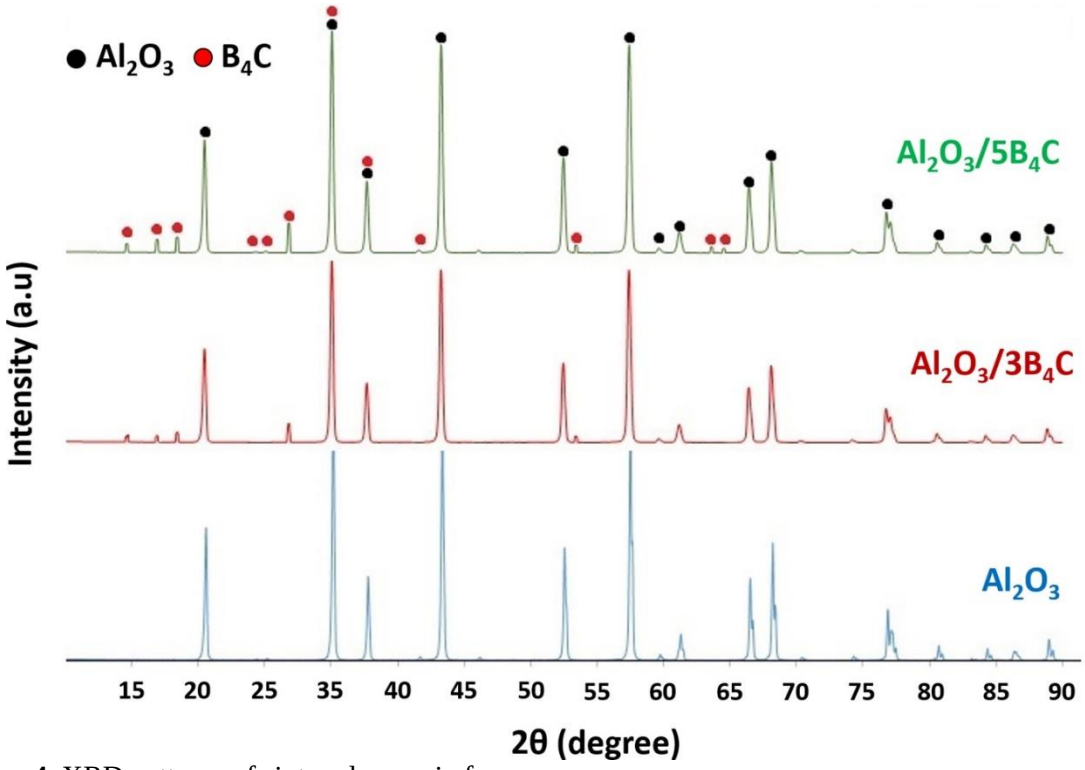

Figure 4. XRD patterns of sintered ceramic foams

3.4. Compressive Strength of Samples

To investigate the characteristics of the ceramic foams that were sintered for 1 hour at 1500 °C, the compressive strength of the samples was evaluated. As shown in Figure 5, the compressive strength of the ceramic foams has enhanced with the addition of B_4C to the Al_2O_3 matrix. When the B_4C content increased to 5 wt.%, the compressive strength of the ceramic foams increased from 1.92 MPa to 2.38 MPa. The improvement can be attributed to the strengthening of sintering necks between the ceramics that form when exposed to the sintering temperature (Oliveira et al., 2006). The increase in B_4C content promotes the formation of stronger necks, resulting in an increase in compressive strength (Chen et al., 2018). These results demonstrate the effectiveness of incorporating B_4C into the Al_2O_3 matrix for improving the mechanical properties of ceramic foams.

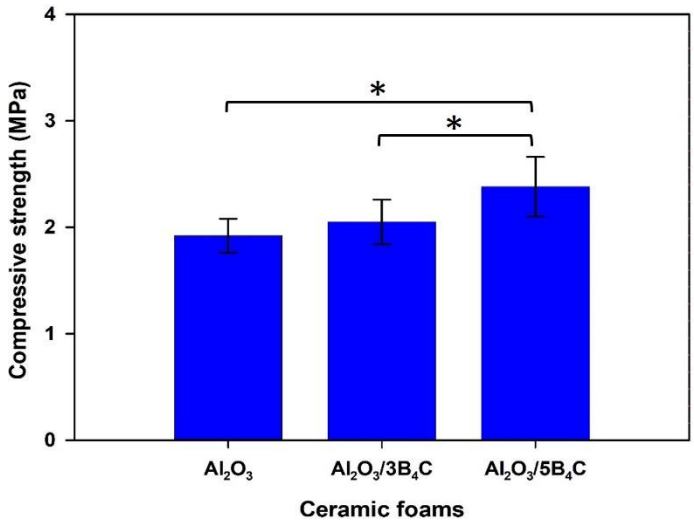

Figure 5. Compressive strength of sintered ceramic foam samples. Values represent the mean and ± SD of six independent experiments. ($p < 0.05$; *Statistically significant differences between groups)

3.5. In Vitro Cytotoxicity Assay

The viability of L929 cells on various ceramic foam samples was evaluated using an MTT assay. Figure 6 shows the representative cell viability (%) of the samples. The results indicated that cells cultured on porous Al_2O_3 ceramic foams with either 3 wt.% B_4C or 5 wt.% B_4C ($p < 0.05$) exhibited significantly higher cell viability than the control groups after 48 hours of incubation, suggesting that porous Al_2O_3 ceramic is beneficial for cell growth. However, cell viability increased with decreasing pore size due to the contamination of B_4C particles with the Al_2O_3 matrix at high temperature. Al_2O_3 is a biocompatible material commonly used in medical implants because of its high mechanical strength and biocompatibility.

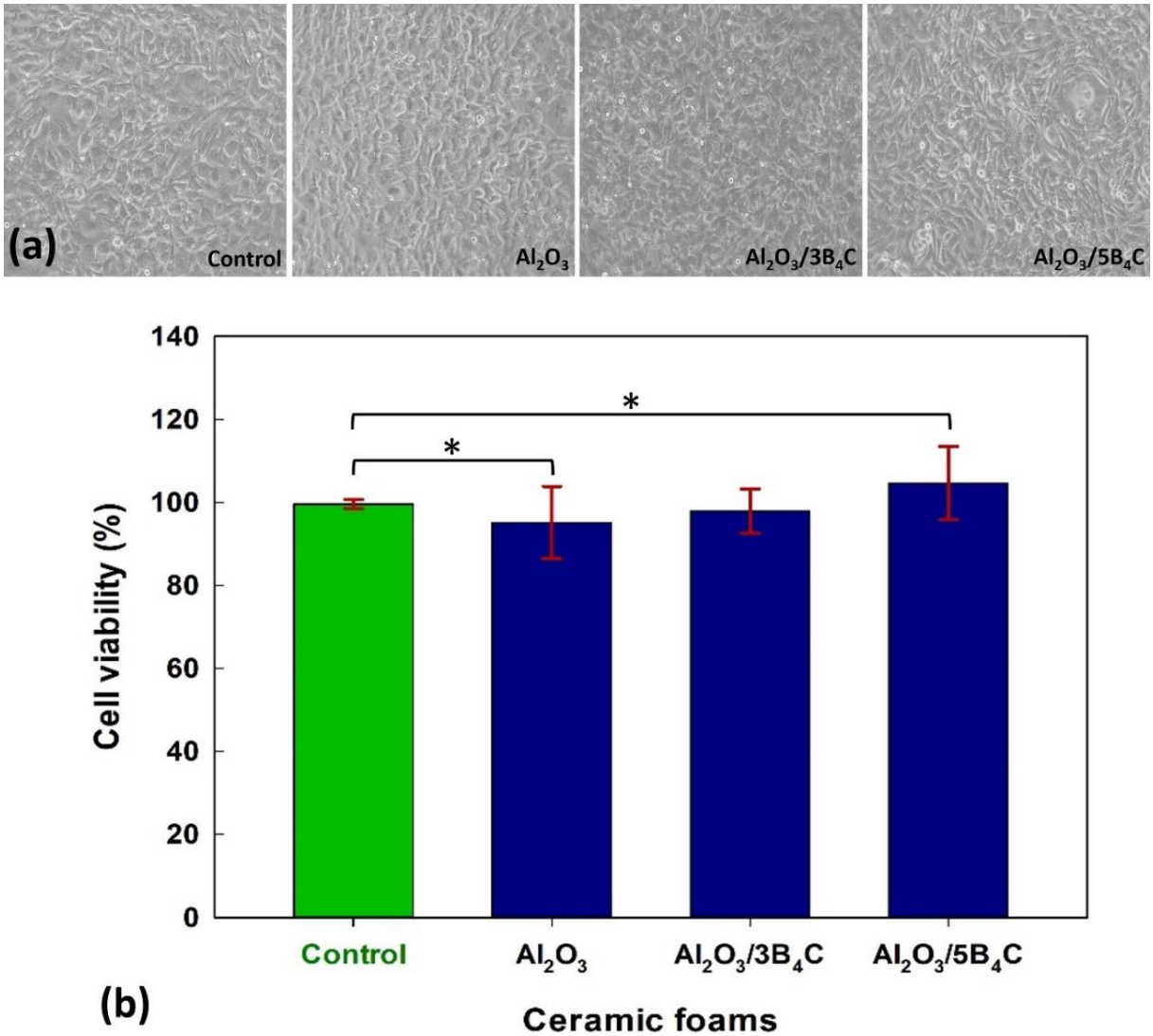

Figure 6. (a) L929 in vitro cell viability real photographs of ceramic foams (x20 magnification), (b) Cell viability diagram by MTT assay. Values represent the mean and ± SD of six independent experiments. ($p < 0.05$; *Statistically significant differences between control groups)

Several studies (Marchi et al., 2009; Karlsson et al., 2003) have shown that cells can attach, proliferate, and differentiate well on pure Al_2O_3 ceramics, but the surface properties of Al_2O_3 ceramics can affect cell behavior and viability. Surface roughness, surface chemistry, and surface energy are all factors that can affect cell attachment and growth. Therefore, the preparation and modification of Al_2O_3 ceramics microstructure with reinforcing additives may have an impact on cell viability. Boron, which is a dopant element, has caught the interest of

biomaterial researchers because of its innate roles in the hard tissues of the human body. Its biological impacts include advancing wound healing, improving the body's response to injuries or infections, altering calcium and bone metabolisms, and exhibiting advantageous effects on central nervous function. Furthermore, it has an impact on the function or presence of hormones such as thyroid hormone, insulin, estrogen, progesterone, and even in vitamin D (Nielsen, 2008; Bose et al., 2013; Dzondo-Gadet et al., 2002). In this study, the ceramics produced by combining with B_4C exhibited no cytotoxic effects in any of the samples. As a matter of fact, it can be concluded that the prepared foams, especially $Al_2O_3/5B_4C$ have great cytocompatibility, which makes ceramic foams suitable to be used in biomedical applications.

4. Conclusions

In conclusion, the addition of 3 wt.% B_4C to 5 wt.% B_4C to the Al_2O_3 matrix during sintering at 1500 °C resulted in ceramic foams with improved mechanical properties and fine microstructure. The interconnectivity and pore size of the resulting ceramic foams make them suitable for use as macroporous scaffolds for facilitating the growth of newly formed hard tissues and cell migration. The X-ray analyses confirmed the effective incorporation of B_4C into the Al_2O_3 matrix, and the compressive strength of the ceramic foams was enhanced with the addition of B_4C. The prepared foams, especially $Al_2O_3/5B_4C$, exhibited great cytocompatibility and no cytotoxic effects, making them suitable for biomedical applications. Overall, the use of B_4C as a reinforcing additive in the microstructure of Al_2O_3 ceramic foams can lead to improvements in their mechanical properties and cytocompatibility, making them a promising material for a range of applications in the fields of biomedicine and tissue engineering.

Acknowledgement

I would like to extend my sincere gratitude to Dr. Ceylan HEPOKUR, a respected faculty member of the Faculty of Pharmacy, for her generous assistance with the in vitro tests conducted in this study. Her expertise and support have been instrumental in the success of this research, and I am truly grateful for her contributions.

Author Contributions

The author confirms sole responsibility for the following: study conception and design, data collection, analysis and interpretation of results, and manuscript preparation.

References

Ahmed, M., Ramadan, R., Afifi, M., Menazea, A. (2020). Au-doped carbonated hydroxyapatite sputtered on alumina scaffolds via pulsed laser deposition for biomedical applications. *Journal of Materials Research and Technology*, 9(4), 8854–8866. https://doi.org/10.1016/j.jmrt.2020.06.006

Akbari beni, H., Alizadeh, M., Ghaffari, M., Amini, R. (2014). Investigation of grain refinement in $Al/Al_2O_3/B_4C$ nano-composite produced by ARB. *Composites Part B: Engineering*, 58, 438–442. https://doi.org/10.1016/j.compositesb.2013.10.037

Barth, R.F., Vicente, M.H., Harling, O.K., Kiger, W., Riley, K.J., Binns, P.J., Wagner, F.M., Suzuki, M., Aihara, T., Kato, I., Kawabata, S. (2012). Current status of boron neutron capture therapy of high grade gliomas and recurrent head and neck cancer. *Radiation Oncology*, 7(1), 1-21. https://doi.org/10.1186/1748-717x-7-146

Bose, S., Fielding, G., Tarafder, S., Bandyopadhyay, A. (2013). Understanding of dopant-induced osteogenesis and angiogenesis in calcium phosphate ceramics. *Trends in Biotechnology*, 31(10), 594–605. https://doi.org/10.1016/j.tibtech.2013.06.005

Bute, A., Jagannath, Kar, R., Chopade, S., Desai, S., Deo, M., Rao, P., Chand, N., Kumar, S., Singh, K., Patil, D., Sinha, S. (2016). Effect of self-bias on the elemental composition and neutron absorption of boron carbide films deposited by RF plasma enhanced CVD. *Materials Chemistry and Physics*, 182, 62–71. https://doi.org/10.1016/j.matchemphys.2016.07.005

Chen, A.N., Li, M., Xu, J., Lou, C.H., Wu, J.M., Cheng, L.J., Shi, Y.S., Li, C.H. (2018). High-porosity mullite ceramic foams prepared by selective laser sintering using fly ash hollow spheres as raw materials. *Journal of the*

European Ceramic Society, 38(13), 4553–4559. https://doi.org/10.1016/j.jeurceramsoc.2018.05.031

Chen, Y.C., Tuan, W.H., Lai, P.L. (2021). Transformation from calcium sulfate to calcium phosphate in biological environment. *Journal of Materials Science: Materials in Medicine*, 32(12), 1-11. https://doi.org/10.1007/s10856-021-06622-7

Dzondo-Gadet, M., Mayap-Nzietchueng, R., Hess, K., Nabet, P., Belleville, F., Dousset, B. (2002). Action of boron at the molecular level effects on transcription and translation in an acellular system. *Biological Trace Element Research*, 85(1), 23–33. https://doi.org/10.1385/bter:85:1:23

Gosset, D., Miro, S., Doriot, S., Moncoffre, N. (2016). Amorphisation of boron carbide under slow heavy ion irradiation. *Journal of Nuclear Materials*, 476, 198–204. https://doi.org/10.1016/j.jnucmat.2016.04.030

Han, Y.S., Li, J.B., Wei, Q.M., Tang, K. (2002). The effect of sintering temperatures on alumina foam strength. *Ceramics International*, 28(7), 755–759. https://doi.org/10.1016/s0272-8842(02)00039-1

Jang, B.K., Enoki, M., Kishi, T., Oh, H.K. (1995). Effect of second phase on mechanical properties and toughening of Al_2O_3 based ceramic composites. *Composites Engineering*, 5(10–11), 1275–1286. https://doi.org/10.1016/0961-9526(95)00069-y

Karlsson, M., Pålsgård, E., Wilshaw, P., Di Silvio, L. (2003). Initial in vitro interaction of osteoblasts with nano-porous alumina. *Biomaterials*, 24(18), 3039–3046. https://doi.org/10.1016/s0142-9612(03)00146-7

Kido, H.W., Ribeiro, D.A., de Oliveira, P., Parizotto, N.A., Camilo, C.C., Fortulan, C.A., Marcantonio, E., da Silva, V.H.P., Muniz Renno, A.C. (2013). Biocompatibility of a porous alumina ceramic scaffold coated with hydroxyapatite and bioglass. *Journal of Biomedical Materials Research Part A*, 102(7), 2072–2078. https://doi.org/10.1002/jbm.a.34877

Luo, J., Shi, X., Li, L., Tan, Z., Feng, F., Li, J., Pang, M., Wang, X., He, L. (2021). An injectable and self-healing hydrogel with controlled release of curcumin to repair spinal cord injury. *Bioactive Materials*, 6(12), 4816–4829. https://doi.org/10.1016/j.bioactmat.2021.05.022

Marchi, J., Delfino, C.S., Bressiani, J.C., Bressiani, A. H.A., Marques, M.M. (2009). Cell proliferation of human fibroblasts on alumina and hydroxyapatite-based ceramics with different surface treatments. *International Journal of Applied Ceramic Technology*, 7(2), 139–147. https://doi.org/10.1111/j.1744-7402.2009.02388.x

Marti, A. (2000). Inert bioceramics (Al_2O_3, ZrO_2) for medical application. *Injury*, 31, D33–D36. https://doi.org/10.1016/s0020-1383(00)80021-2

Mirzayev, M.N., Demir, E., Mammadov, K.F., Sukratov, V.A., Jabarov, S.H., Biira, S., Asgerov, E.B., Abdurakhimov, B.A., Tuğrul, A.B. (2020). Amorphisation of boron carbide under gamma irradiation. *Pramana*, 94(1), 1-8. https://doi.org/10.1007/s12043-020-01980-3

Mortensen, M., Sørensen, P., Björkdahl, O., Jensen, M., Gundersen, H., Bjørnholm, T. (2006). Preparation and characterization of Boron carbide nanoparticles for use as a novel agent in T cell-guided boron neutron capture therapy. *Applied Radiation and Isotopes*, 64(3), 315–324. https://doi.org/10.1016/j.apradiso.2005.08.003

Naga, S.M., El-Kady, A.M., El-Maghraby, H.F., Awaad, M., Detsch, R., Boccaccini, A.R. (2013). Novel porous Al_2O_3-SiO_2-TiO_2 bone grafting materials: Formation and characterization. *Journal of Biomaterials Applications*, 28(6), 813–824. https://doi.org/10.1177/0885328213483634

Nielsen, F.H. (2008). Is boron nutritionally relevant? *Nutrition Reviews*, 66(4), 183–191. https://doi.org/10.1111/j.1753-4887.2008.00023.x

Oliveira, F.C., Dias, S., Vaz, M.F., Fernandes, J.C. (2006). Behaviour of open-cell cordierite foams under compression. *Journal of the European Ceramic Society*, 26 (1–2), 179–186. https://doi.org/10.1016/j.jeurceramsoc.2004.10.008

Öksüz, K.E., Kurt, B., Şahin İnan, Z.D., Hepokur, C. (2023). Novel bioactive glass/graphene oxide-coated surgical sutures for soft tissue regeneration. *ACS Omega*, 8(24), 21628–21641. https://doi.org/10.1021/acsomega.3c00978

Öksüz, K.E. (2019). Effect of composition and sintering temperature on the structure and

properties of porous bioactive glass scaffolds, *Chiang Mai Journal of Science*, 46(3), 568-578. http://epg.science.cmu.ac.th/ejournal/

Öksüz, K.E., Özkaya, N.K., İnan, Z.D.A., Özer, A. (2021). Novel natural spider silk embedded electrospun nanofiber mats for wound healing. *Materials Today Communications*, 26, 101942. https://doi.org/10.1016/j.mtcomm.2020.101942

Öksüz, K., Özer, A. (2017). Effect of yttria on the phase formation and sintering of HA-Al_2O_3 biocomposites. *Acta Physica Polonica A*, 131(3), 576–580. https://doi.org/10.12693/aphyspola.131.576

Özer, A., Öksüz, K. (2019). The effect of yttrium oxide in hydroxyapatite/aluminum oxide hybrid biocomposite materials: Phase, mechanical and morphological evaluation. *Materialwissenschaft und Werkstofftechnik*, 50(11), 1382–1390. https://doi.org/10.1002/mawe.201800141

Silva, J.R.S., Santos, L.N.R.M., Farias, R.M.C., Sousa, B.V., Neves, G.A., Menezes, R.R. (2022). Alumina applied in bone regeneration: Porous α-alumina and transition alumina. *Cerâmica*, 68(387), 355–363. https://doi.org/10.1590/0366-69132022683873335

Sulyman, M., Kucinska-Lipka, J., Sienkiewicz, M., Gierak, A. (2021). Development, characterization and evaluation of composite adsorbent for the adsorption of crystal violet from aqueous solution: Isotherm, kinetics, and thermodynamic studies. *Arabian Journal of Chemistry*, 14(5), 103115. https://doi.org/10.1016/j.arabjc.2021.103115

Suri, A.K., Subramanian, C., Sonber, J.K., Murthy, T. S.R.C. (2010). Synthesis and consolidation of boron carbide: a review. *International Materials Reviews*, 55(1), 4–40. https://doi.org/10.1179/095066009x12506721665211

Tan, W., Jiang, X., Shao, Z., Sun, H., Song, T., Luo, Z. (2020). Fabrication and mechanical properties of α-Al_2O_3 whisker reinforced cu-graphite matrix composites. *Powder Technology*, 375, 124–135. https://doi.org/10.1016/j.powtec.2020.07.105

Tian, Y. (1999). A Review of: Handbook of refractory carbides and nitrides: properties, characteristics, processing, and applications. *Materials and Manufacturing Processes*, 14(2), 300–301. https://doi.org/10.1080/10426919908907558

Turnbull, G., Clarke, J., Picard, F., Riches, P., Jia, L., Han, F., Li, B., Shu, W. (2018). 3D bioactive composite scaffolds for bone tissue engineering. *Bioactive Materials*, 3(3), 278–314. https://doi.org/10.1016/j.bioactmat.2017.10.001

Werheit, H. (2016). Boron carbide: Consistency of components, lattice parameters, fine structure and chemical composition makes the complex structure reasonable. *Solid State Sciences*, 60, 45–54. https://doi.org/10.1016/j.solidstatesciences.2016.08.006

Wu, R., Li, Y., Shen, M., Yang, X., Zhang, L., Ke, X., Yang, G., Gao, C., Gou, Z., Xu, S. (2021). Bone tissue regeneration: The role of finely tuned pore architecture of bioactive scaffolds before clinical translation. *Bioactive Materials*, 6(5), 1242–1254. https://doi.org/10.1016/j.bioactmat.2020.11.003

Xue, N., Ding, X., Huang, R., Jiang, R., Huang, H., Pan, X., Min, W., Chen, J., Duan, J.A., Liu, P., Wang, Y. (2022). Bone Tissue Engineering in the Treatment of Bone Defects. *Pharmaceuticals*, 15(7), 879. https://doi.org/10.3390/ph15070879

Yoshie Ishikawa, T.I. (2014). Boron carbide particle as a boron compound for boron neutron capture therapy. *Journal of Nuclear Medicine and Radiation Therapy*, 5(2), 1-5. https://doi.org/10.4172/2155-9619.1000177

Zheng, Z., Chen, B., Fritz, N., Gurumukhi, Y., Cook, J., Ates, M.N., Miljkovic, N., Braun, P.V., Wang, P. (2020). The Impact of non-uniform metal scaffolds on the performance of 3D structured silicon anodes. *Journal of Energy Storage*, 30, 101502. https://doi.org/10.1016/j.est.2020.101502